Influences of piles on the ground vibration considering the train-track-soil dynamic interactions

Li, Ting; Su, Qian; Kaewunruen, Sakdirat

DOI:
10.1016/j.compgeo.2020.103455

Influences of piles on the ground vibration considering the train-track-soil dynamic interactions

Ting Li[a,b,c], Qian Su[a,b], Sakdirat Kaewunruen[c,*]

[a] *School of Civil Engineering, Southwest Jiaotong University, Chengdu 610031, China*

[b] *Key Laboratory of High-Speed Railway Engineering, Ministry of Education, Southwest Jiaotong University, Chengdu 610031, China*

[c] *School of Engineering, University of Birmingham, Birmingham B15 2TT, UK*

[*]Correspondence should be addressed to Sakdirat Kaewunruen (s.kaewunruen@bham.ac.uk).

Abstract: High-speed trains can induce significant amplification of dynamic responses of components in railway tracks especially when the train travels at the so-called 'critical speed'. Based on a critical literature review, most previous studies with respect to train-track-soil interactions have merely been focused on the simplified natural ground vibrations. Accordingly, there exists no investigation into the influences of piles on the ground responses despite the fact that the pile-reinforced ground improvement has been widely adopted in soft soil regions for high-speed railway with slab track systems. In order to highlight the influences of piles on ground vibrations, a 3D fully coupled train-track-soil model has been developed based on the multi-body simulation principle, finite element theory, and perfectly matched layers method using LS-DYNA, in which the dynamic material properties of slab tracks have been adopted. This model has been validated by comparing its results of ground vibrations and train-track interactions with field-test results. This is thus the world's first to investigate the critical speeds of slab-track railway with natural and pile-reinforced ground improvement. The dynamic displacements, vibration velocities, and dynamic stresses of soils with natural and pile-reinforced grounds have then been evaluated under normal and critical train speeds. The accelerations of car body and dynamic impact factors with the increasingly train speed have also been presented. The piles influences on the wave propagations in the soils have been highlighted. The insight from this study provides a new and better understanding of ground vibrations in high-speed railway systems using slab tracks in practice.

Keywords: pile effect; ground vibration; critical speed; train-track-soil interactions; perfectly matched layers; wave propagation

1. Introduction

As one of the most sustainable developments for ground transportation, the high-speed railway has been developed rapidly all over the world over the recent several decades [1-3]. The French TGV has reached a record top speed of 574.8 km/h. The Chinese ‘Fuxing’ train is traveling at a speed of 350 km/h in numerous rail networks in China. These high-speed trains can impart higher dynamic forces to rail infrastructures and result in an elevated vibration level for the coupled train-track-soil system [4]. In order to meet the requirements for the high-speed rail system, the slab tracks, highly-compacted subgrade, and pile-reinforced ground are customarily adopted in high-speed railways [5-7], as illustrated in Figure 1.

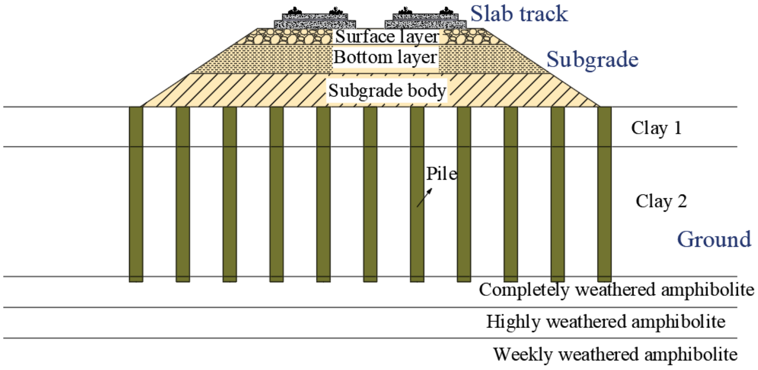

Figure 1 Cross-section of a high-speed railway (adopted from Ref. [7])

The ground-borne vibration induced by the train-track-soil dynamic interactions has received increasing attention recently [8-10]. According to previous studies, high-speed trains traveling on soft soils can significantly increase the vibration level especially when the train moves at the so-called ‘critical speed’, at which the train induces a resonance-like phenomenon [4, 11]. The critical speed depends typically on the Rayleigh wave velocity of soft soils. The measured dynamic displacement of the track can be three times the static value when the train speed is close to the Rayleigh wave velocity at the well-known railway site at Sweden [8, 9]. Many studies have been conducted to investigate the ground vibration of ballasted-track railway under normal and critical train speeds, including the propagation of Rayleigh wave in the soils [12, 13], development of the constitutive model of nonlinear soil with large deformation [14, 15], influence of soil properties on the ground vibration [16, 17], evaluation of the environmental ground vibration [18, 19], and so on. Most previous studies have merely considered the natural ground with soft soils. However, the pile-reinforced ground improvement is widely adopted in soft soil region in high-speed railways since it can significantly reduce both total and differential settlement of soils [20, 21], bringing about an excellent long-term performance during the operation of railways [22, 23]. As the piles can increase the stiffness of soft ground, the vibration responses of railway with pile-reinforced ground will be different from the responses with natural ground. In addition, the previous studies have customarily considered the ground vibration under ballasted track [11, 15-18]. However, the use of slab track is getting prevailing in high-speed railways nowadays [5, 6, 24]. The slab track can also prompt different railway vibration responses. It is crucial to highlight the influences of piles on the ground vibration in high-speed railway with slab tracks.

The high-speed train, slab track, multi-layered subgrade, and pile-reinforced ground are a coupled dynamic interaction system. With the development of computer science, numerical simulation has become an efficient technique to investigate railway vibration responses [3, 25, 26]. Although previous researchers such as Thach et al. [27] and Tang et al. [28] developed a numerical model to investigate the vibration responses of railway with pile-reinforced ground, they just simplified the vehicle as the moving load, which is unable to simulate the dynamic excitation effect induced by the train-track interactions with the roughness of rail surface. The 2D and 2.5D models have also been developed to analyze the ground vibration responses but these models are still limited in scope due to the plane stress/strain assumptions. In order to overcome these limitations, Kouroussis et al. [16, 17] and Connolly et al. [29, 30] developed a 3D coupled train-track-soil numerical model to study the ground vibration responses. However, they just simulated the natural ground without considering any improvements in soft soils.

Considering previous studies have merely investigated the natural-ground vibration under ballasted track, a 3D fully coupled train-track-soil model has been developed using LS-DYNA to investigate the piles influences on the ground vibration responses in high-speed railway with slab tracks. The critical speeds of the railway with natural and pile-reinforced grounds have been highlighted firstly. The vibration responses of the railway have then been evaluated. Besides, it is original to discuss the influences of piles on the wave propagations in the soils with natural and pile-reinforced grounds. This study could bring an insightful and better understanding of the vibration responses of high-speed railway with pile-reinforced ground and slab track for the design, operation, and maintenance for the rail system in practice.

2. Modeling of the train-track-soil dynamic interactions

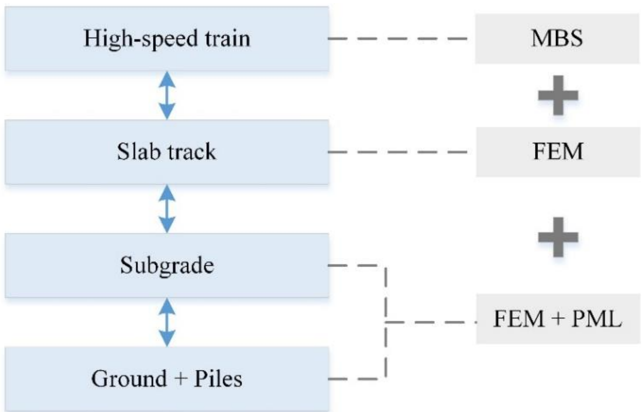

Figure 2 Coupling of the train-track-soil system

A novel 3D coupled train-track-soil model is developed using LS-DYNA to investigate the influences of piles on the ground vibration in high-speed railway with slab tracks. The high-speed train is simulated based on the multi-body simulation (MBS) principle, and the slab track is developed based on the finite element modeling (FEM) theory. Besides, the subgrade and pile-reinforced ground are simulated based on the FEM theory together with the Perfectly Matched Layers (PML) method, as illustrated in Figure 2.

2.1 Modeling of the high-speed train and slab track

The coupled train-track-soil dynamic system is developed based on a typical cross-section in Beijing-Shanghai high-speed railway in China [7]. The vehicle commonly operated on this section is the China Railway High-speed (CRH) 380 Electric Multiple Unit (EMU) train. In this simulation model, the vehicle consists of one car body, two bogies, four wheelsets, and two stage-suspension systems, as shown in Figure 3. The car body, bogies, and wheelsets are simplified as the rigid-bodies with shell and beam elements. These multi-rigid-bodies are connected by the springs and dashpots. As the vertical vibration is the primary excitation to the infrastructures, the vertical degrees of freedom (DOF) of the vehicle are considered in this model. The vehicle has totally 10 DOF including the vertical and pitch motion of car body (Z_c, β_c), the vertical and pitch motion of bogies (Z_{bi}, β_{bi} $i=1,2$), and the vertical motion of wheelsets (Z_{wi} $i=1,...,4$).

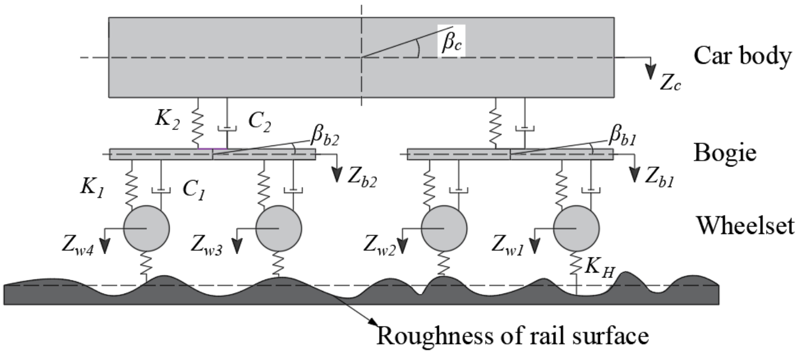

Figure 3 Simulation of the vehicle

The China Railway Track System (CRTS) II slab track is adopted in this railway. It consists of rail, rail pads, concrete slab, cement asphalt (CA) mortar layer, and concrete base [31]. The rail is simulated as the Euler beam, which is supported by the discrete springs and dashpots to represent the rail pads. The concrete slab, CA mortar, and concrete base are simulated as solid elements.

The contact between wheel and rail is simulated based on the Hertz contact theory. The wheel-rail contact force can be calculated automatically by LS-DYNA based on the following equation:

$$F = K_H \times (Z_w - Z_r - \delta) \tag{1}$$

Where K_H is the vertical stiffness of the wheel-rail contact spring, K_H =1.325×10^9 N/m in this study [32]; Z_w is the vertical displacement of the wheel; Z_r is the vertical displacement of the rail; and δ is the roughness of rail surface.

The Germany high-speed low disturbance irregularity is used to excite the wheel-rail contact. The power spectrum density (PSD) function of the roughness is calculated as follows:

$$S_v(\Omega) = \frac{A_v \Omega_c^2}{(\Omega^2 + \Omega_r^2)(\Omega^2 + \Omega_c^2)} \tag{2}$$

Where A_v is the roughness constant ($A_v = 4.032\times10^{-7}\ \mathrm{m}^2\cdot\mathrm{Rad/m}$); Ω_c and Ω_r are the cutoff frequency ($\Omega_c = 0.8246$ rad/m, $\Omega_r = 0.0206$ rad/m); and Ω is the spatial frequency of the roughness. The PSD function can be transformed into vertical roughness along the longitudinal distance of the track using a time-frequency transformation technique, as shown in Figure 4.

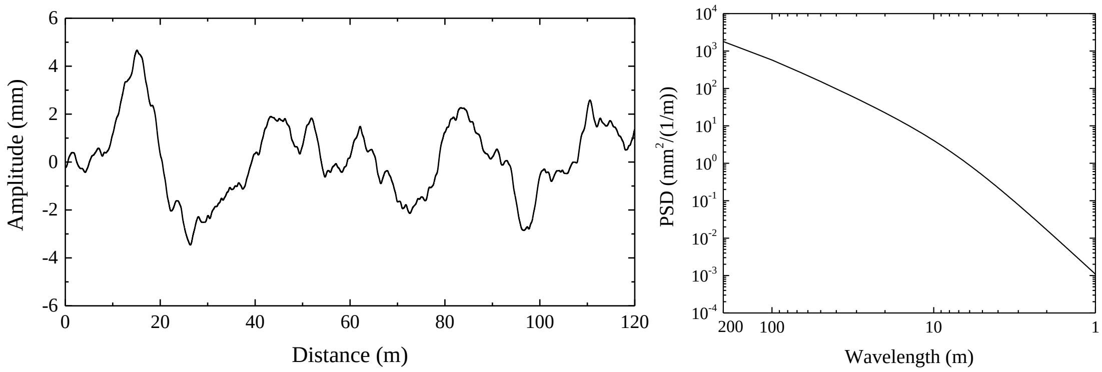

(a) Roughness with distance (b) PSD with wavelength

Figure 4 The roughness of rail surface

The material properties of the CRH380 EMU Train and CRTS II slab track are shown in Table 1. Since most previous studies adopted static material properties of slab track despite the fact that the actual loads from high-speed trains onto slab tracks are dynamic excitation, the dynamic material properties of CRTS II slab track are used in this model in order to obtain a more realistic vibration response. The stiffness of rail pads is determined by the dynamic value, and the moduli of elasticity of concrete slab, CA mortar, and concrete base are considered as the strain-rate dependent values [33, 34].

Table 1 Properties of the vehicle and slab track

Properties	Values
CRH380 EMU Train	
Mass of the car body (kg)	40,000
Mass of the bogie (kg)	3,200
Mass of the wheelset (kg)	2,400
Inertia of pitch motion of the car body(kg.m^2)	5.47×10^5
Inertia of pitch motion of the bogie(kg.m^2)	6,800
Primary suspension stiffness (N/m)	1.04×10^6
Primary suspension damping (N.s/m)	5×10^3
Secondary suspension stiffness (N/m)	4×10^5
Secondary suspension damping (N.s/m)	6×10^3
CRTS II slab track	
Mass density of the rail (kg/m^3)	7,830

Modulus of elasticity of the rail (Pa)	2.059×10^{11}
Poisson's ratio of the rail	0.3
Stiffness of the rail pads (N/m)	5.0×10^{7} (dynamic stiffness)
Damping of the rail pads (N.s/m)	7.5×10^{4}
Mass density of the concrete slab (kg/m^3)	2,500
Modulus of elasticity of the concrete slab (Pa)	3.6×10^{10} (reference static value, strain-rate dependent)
Poisson's ratio of the concrete slab	0.2
Mass density of the CA mortar (kg/m^3)	1,900
Modulus of elasticity of the CA mortar (Pa)	7×10^{9}(reference static value, strain-rate dependent)
Poisson's ratio of the CA mortar	0.2
Mass density of the concrete base (kg/m^3)	2,400
Modulus of elasticity of the concrete base (Pa)	2.55×10^{10}(reference static value, strain-rate dependent)
Poisson's ratio of the concrete base	0.2

2.2 Modeling of the soil

The subgrade consists of three layers in the Beijing-Shanghai high-speed railway: surface layer, bottom layer, and subgrade body. The ground consists of five layers: clay 1, clay 2, completely weathered amphibolite, highly weathered amphibolite, and weekly weathered amphibolite, as illustrated in Figure 1. The soils are simulated as viscoelastic material using solid elements. In addition, since the amphibolite is a type of rock, and the stiffness of amphibolite is much higher than that of clay [7], the three layers of the amphibolite are not developed in the model, and the fixed boundary is set at the bottom of the second layer of ground instead.

To prevent spurious wave reflections from the truncated boundary, perfectly matched layers (PML) method, which is the most efficient infinite boundary, is used in this simulation model. PML is set parallel to the FEM domain, and it can perfectly attenuate the outgoing waves and then reflect them with arbitrarily small amplitudes back to the FEM domain [35, 36], as illustrated in Figure 5.

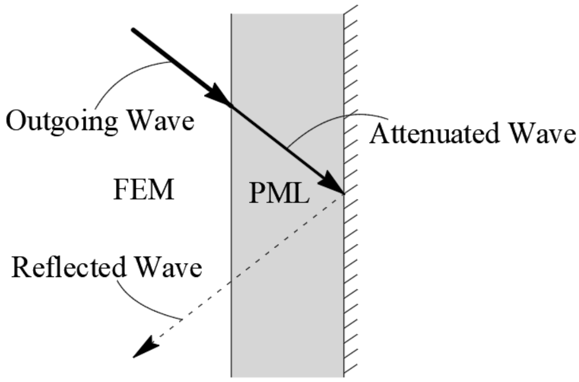

Figure 5 Absorbing boundary of PML

The material properties of soils are measured from the section of the Beijing-Shanghai high-speed railway, as shown in Table 2. Note that most in-site tests cannot give precise information on the damping of internal soils. In order to minimize the gap between the experimental and numerical dynamic responses of the soil, the Rayleigh damping of soil is usually used in the simulation models [29, 30]. The damping matrix is defined as:

$$[\mathbf{C}] = \alpha[\mathbf{M}] + \beta[\mathbf{K}] \tag{3}$$

Where $\mathbf{M}$ and $\mathbf{K}$ are the mass and stiffness matrix of the whole FEM model, respectively; and α and β are the coefficients. In this model, $\alpha = 0$ and $\beta = 0.0002$ [17].

Table 2 Properties of soils and pile (c_p : P wave velocity; c_s : S wave velocity; c_R: Rayleigh wave velocity)

Components	Depth (m)	Density (kg/m^3)	Modulus of elasticity (MPa)	Poisson's ratio	c_p (km/h)	c_s (km/h)	c_R (km/h)
Surface layer of subgrade	0.4	2300	200	0.25	1162.90	671.40	616.08
Bottom layer of subgrade	2.3	1950	150	0.35	1264.91	607.64	567.58
Subgrade body	2	2100	110	0.3	955.95	510.98	473.24
First layer of ground	2.4	1900	42	0.3	621.01	331.94	307.43
Second layer of ground	13.1	2010	83	0.36	948.39	443.57	415.00
Pile	15.5	2200	7000	0.2	-	-	-

2.3 Modeling of the pile

The cement fly-ash gravel (CFG) piles are adopted in the soft soils in Beijing-Shanghai high-speed railway to improve the serviceability of the ground [7]. The length of the piles is 15.5 m. The diameter and spacing of the piles are 0.5 m and 1.8 m, respectively.

In the simulation model, the beam element is used to simulate piles to improve the computational efficiency, and the shared node method is adopted for the piles and soils. Unlike the cyclic dynamic loads, the monotonic train loads cannot induce the consolidation of soft soils, and the deferential deformation between piles and soils is relatively small, so the friction between piles and soils is neglected in this model [37, 38]. The material properties of the piles are shown in Table 2.

2.4 Computational implementation

The dimension of the whole model is 120 m × 130 m × 15.5 m, as illustrated in Figure 6. It is noted that the Beijing-Shanghai high-speed railway line is a double-track railway, indicating that the model cannot be developed as a half model from the center of the railway since the dynamic train load is not always symmetrical.

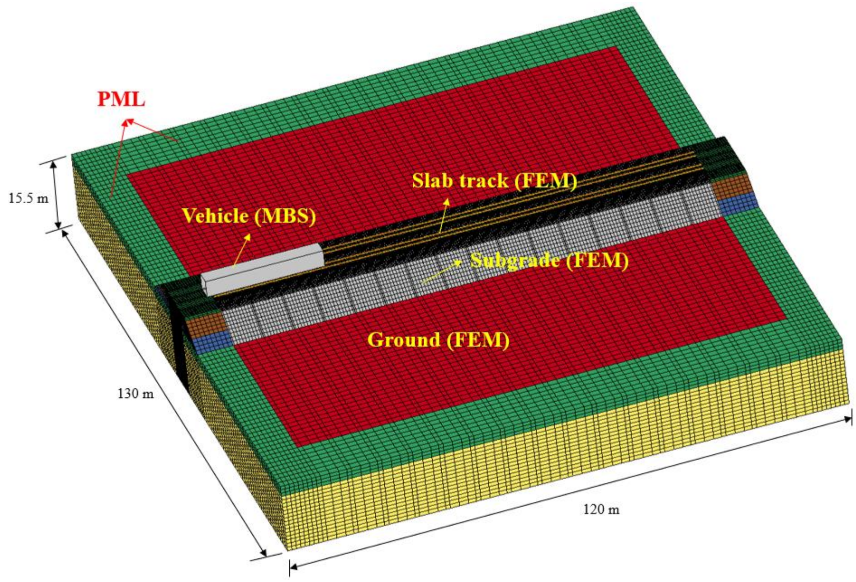

(a) Whole model

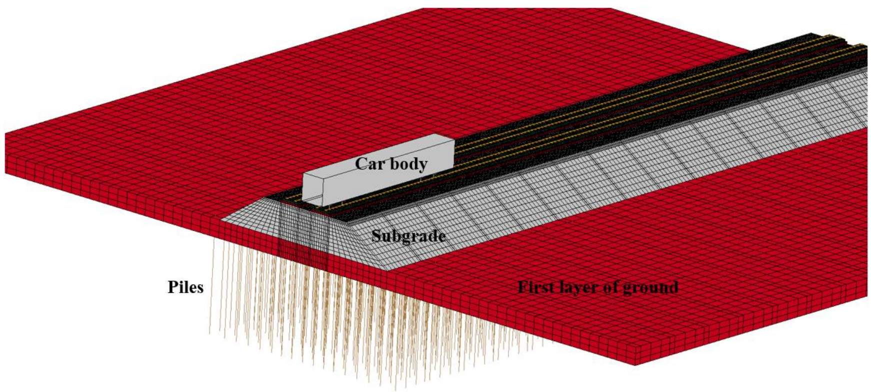

(b) Pile-reinforced ground model

Figure 6 Numerical model in LS-DYNA

The wheel-rail contact is developed using the built-in keywords in LS-DYNA: *RAIL_TRACK and *RAIL_TRAIN. In these keywords, a realistic roughness of rail surface and a contact stiffness can be defined by users.

Eight layers of solid elements are created around the soil for the PML elements, which are defined by the material: *MAT_PML_ELASTIC. The PML elements have identical properties to the FEM elements.

As the dynamic material properties of the slab track are considered, the keyword *MAT_STRAIN_RATE_DEPENDENT_PLASTICITY is used to describe the strain-rate dependent modulus of elasticity.

The model is developed as two types: model with natural ground and model with pile-reinforced ground, to investigate the influences of piles on the ground vibration. The natural ground model has 399,386 elements, and the pile-reinforced ground model has 419,798 elements, including beam elements, shell elements, solid elements, springs, and dashpots.

The vehicle is set to travel at a constant speed over the rail after the dynamic relaxation. The explicit central difference method is used to integrate the equations of motion of the coupled train-track-soil system by LS-DYNA with a time step of 1.23×10^{-5} s.

3. Model validation

3.1 Acceleration of ground

The acceleration of the environmental ground has been measured in the Beijing-Shanghai high-speed railway with a train speed of 300 km/h [7]. This model can thus be validated by comparing the acceleration from the numerical model against the field-test results, as illustrated in Figure 7.

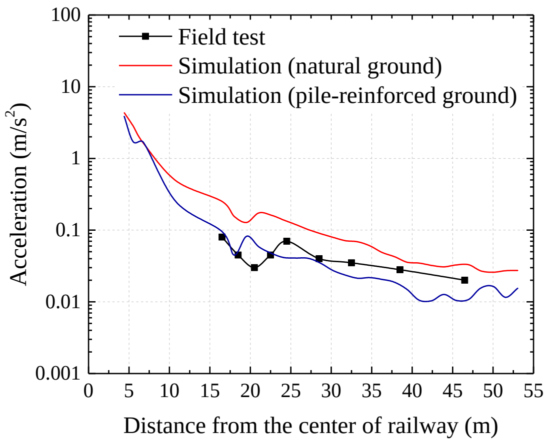

(a) Vertical acceleration

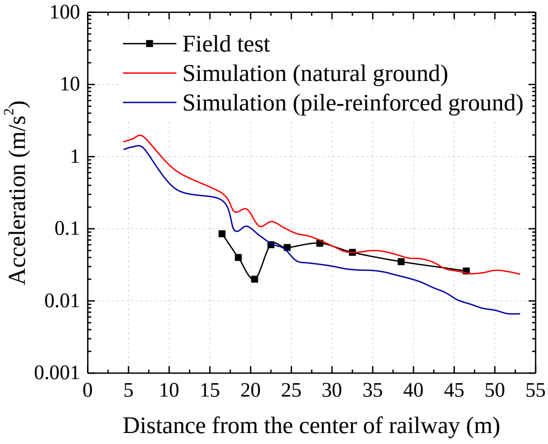

(b) Lateral acceleration

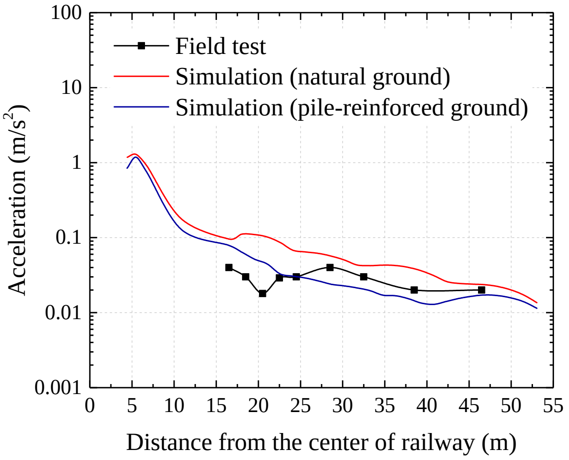

(c) Longitudinal acceleration

Figure 7 Validation results of ground vibration

The accelerations of soils from the numerical simulations are in good agreement with the field-test results. Although there are differences between these results due to some assumptions of numerical models, the differences are considerably small. The amplitudes in vertical, lateral, and longitudinal directions are less than 0.3 m/s^2 when the distance is longer than 16.5 m. The acceleration in natural ground is higher than that in pile-reinforced ground, indicating the piles can attenuate the ground vibration responses. Therefore, the numerical model developed in this study can predict the ground vibration responses for railways in practice.

3.2 Train-track interactions

The wheel-rail contact responses have not been obtained from the Beijing-Shanghai high-speed railway. In order to validate the train-track interactions, the calculated wheel-rail contact responses are compared with the field-test results from the Suining-Chongqing railway, which is constructed to investigate the dynamic performance of vehicle and slab tracks. The material properties of vehicle and slab track are adopted according to this railway [39].

Table 3 Validation results of train-track dynamic interactions

	Field-test results [39]	Simulation results from Cai et al. [40]	Simulation results from this study
Wheel-rail contact force (kN)	81-116	98.7	96.3
Rail pad force (kN)	14.4-65.8	37.648	35.1
Displacement of the rail (mm)	0.3-0.88	0.827	0.863

The train-track interactions obtained from the field test, simulation model from Cai et al., and simulation model from this study are compared in Table 3. The simulation results from this model are considered to be within an acceptable range relative to the field-test results, and also match with the simulation results from Ref.[40]. In sum, the train-track interactions established in this study also exhibit a good agreement with the field-test results and other simulation results.

4. Results

In order to investigate the effects of piles on the ground vibration, the critical speed of the Beijing-Shanghai high-speed slab-track railway is calculated from the natural and pile-reinforced ground models firstly. The vibration responses of soils are then analyzed under normal and critical speeds. The train-track dynamic interactions are also investigated for comparisons under natural and pile-reinforced ground cases.

4.1 Critical speed

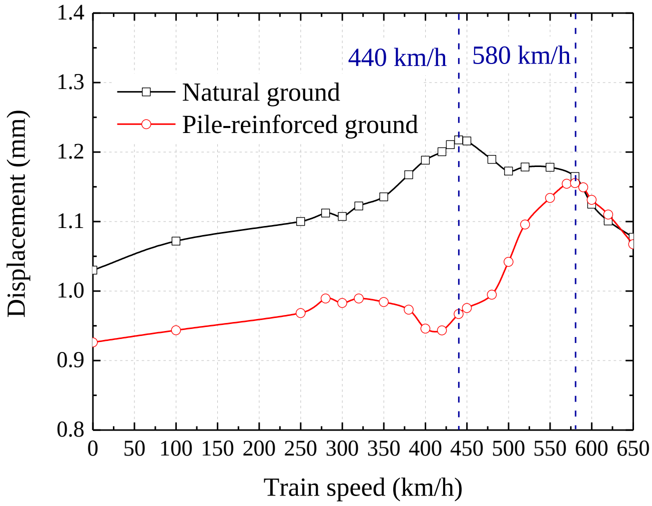

Figure 8 Maximum displacement of rail with train speed

The maximum dynamic displacements of rail in natural and pile-reinforced ground cases are shown in Figure 8 when the train speed is increased from 0 km/h to 650 km/h. Although a speed of 650 km/h is much higher than the normal operational train speed (≤ 400 km/h), this study is aimed at demonstrating the critical speeds of the high-speed slab-track railway with natural and pile-reinforced ground.

In Figure 8, the displacements from the natural ground case are much higher than those from the pile-reinforced ground case. Therefore, the pile exhibits a significant attenuation effect on the ground vibration responses before the train achieves a speed of 580 km/h.

When the piles are not considered, the critical speed of the slab-track railway is around 440 km/h. Unlike the amplification effect in the ballasted track [8, 9], the increased displacement in slab track at critical speed is insignificant, which is rather similar to a previous study in Ref. [41]. The displacement is increased by 18.4% from 1.03 mm (at 0 km/h) to 1.22 mm (at 440 km/h). It is likely that slab track exhibits a higher global track stiffness than conventional ballasted track, leading to a smaller amplification of resonance-like phenomenon. In addition, the critical speed in this model, 440 km/h, is not close to Rayleigh wave velocities of any soil layers. In previous studies, the subgrade is normally simplified as the isotropic material, so the critical speed is normally determined by the Rayleigh wave velocity of the subgrade or the first layer of ground [8, 9, 41]. However, there are five layers of soils in this study. The trapezoidal three layers of subgrade and five types of soil properties make the propagation of both surface and body waves complicated.

When the piles are considered, the critical speed is increased to 580 km/h. The displacement is increased by 25% from 0.926 mm (at 0 km/h) to 1.16 mm (at 580 km/h). This amplification effect is more significant than that of natural ground case. Also, this critical speed is still generated by five layers of soils but with higher stiffness.

It is also noticeable that the critical speed of slab-track railway is much higher than the current operational train speed whether the piles are considered or not. Besides, the amplification effect at critical speed is insignificant, indicating the slab track possesses an excellent dynamic performance.

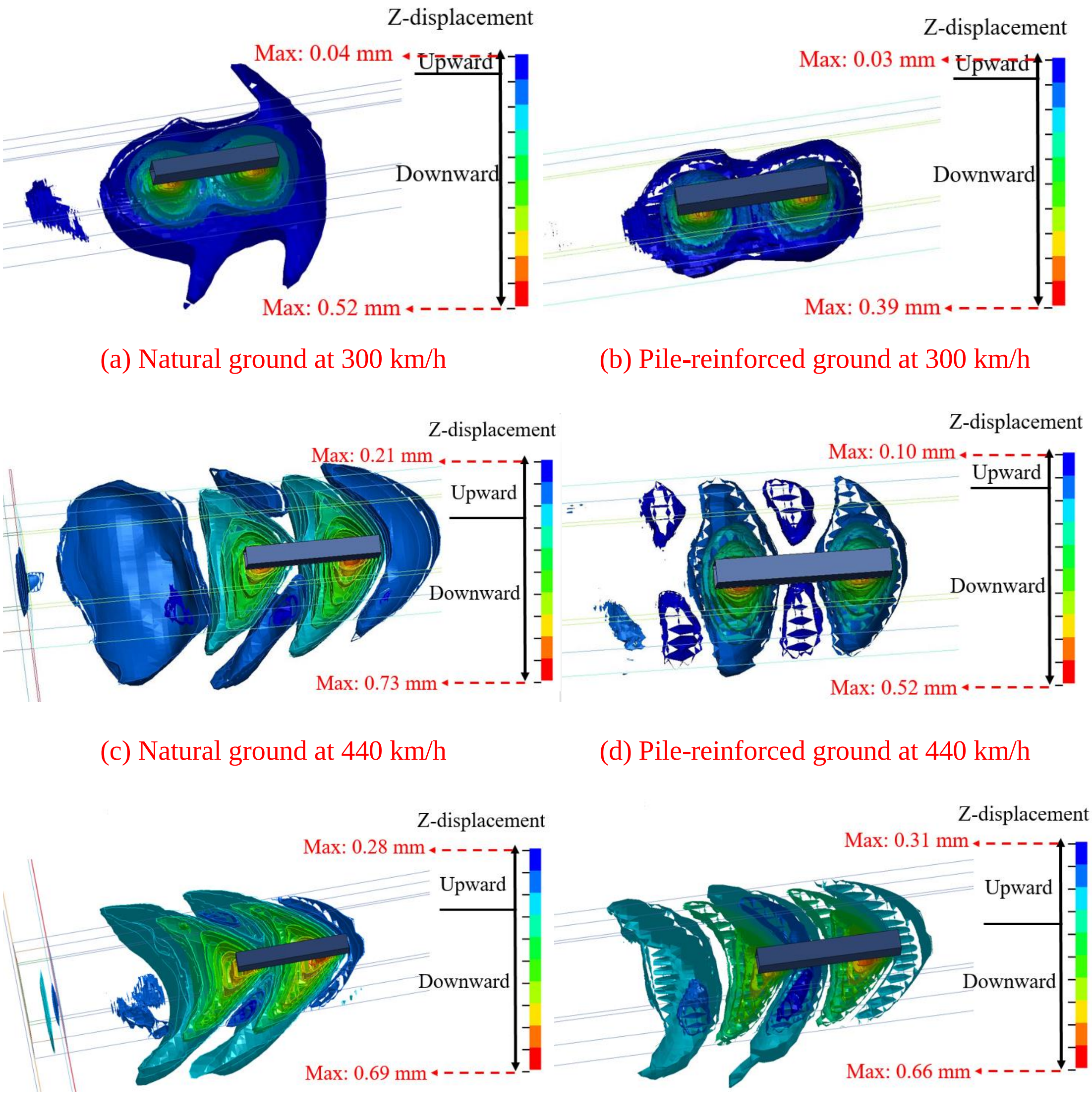

(a) Natural ground at 300 km/h (b) Pile-reinforced ground at 300 km/h

(c) Natural ground at 440 km/h (d) Pile-reinforced ground at 440 km/h

(e) Natural ground at 580 km/h (f) Pile-reinforced ground at 580 km/h

Figure 9 Contours of displacement of the soils

The contours of displacement of soils under three train speeds (normal speed and two critical speeds) are illustrated in Figure 9. When the train speed is 300 km/h, the contours of the dynamic displacements are concentrated in a small range of soils. The piles can significantly reduce the downward displacement but have no obvious influence on the upward displacement. When the train travels at 440 km/h, the Mach cone phenomenon, which is analogous to a boat moving through the water, can be observed in the natural ground case. This phenomenon cannot be observed in pile-reinforced ground case at 440 km/h. In addition, since this speed is the critical speed for natural ground case, both upward and downward displacements of soils are higher than those of pile-reinforced ground case. When the train speed reaches to 580 km/h, the piles have no obvious influence on the amplitudes of the displacements, but the Mach cone phenomenon can be observed in both natural and pile-reinforced ground cases.

4.2 Dynamic responses of soils

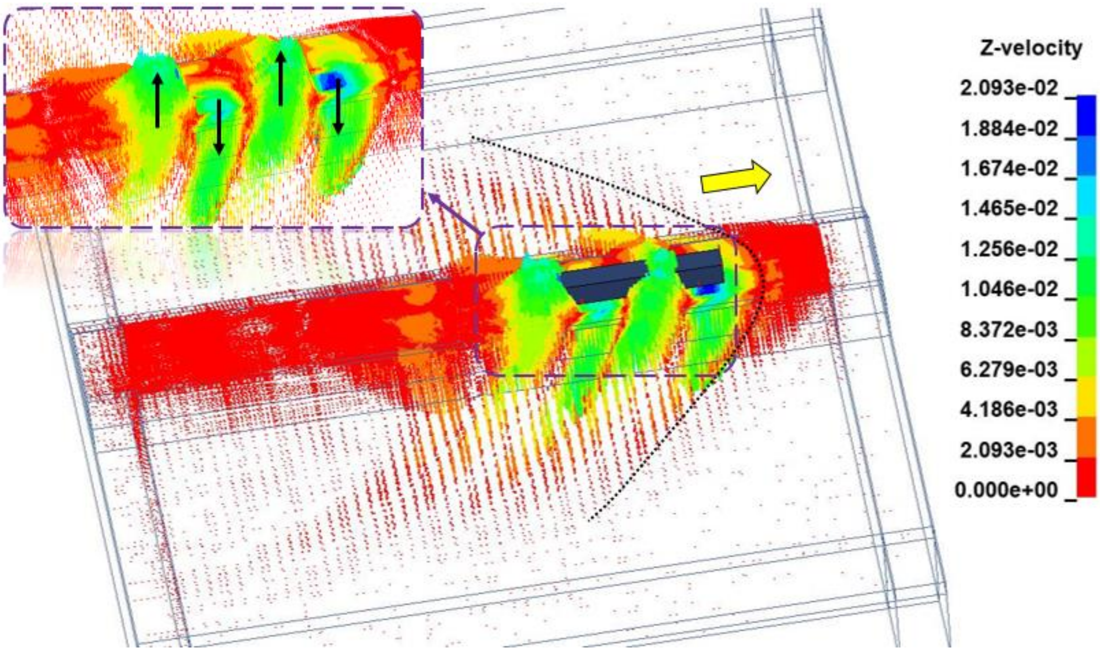

(a) Natural ground

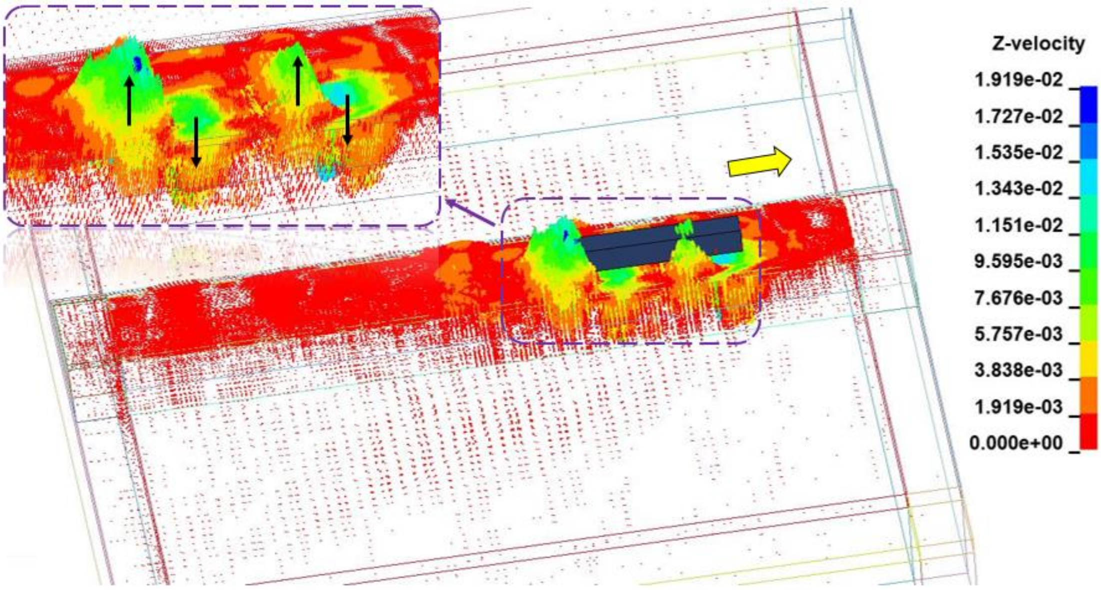

(b) Pile-reinforced ground

Figure 10 Vectors of the vertical velocity of soils

The vectors of the vertical velocity of soils with natural and pile-reinforced ground are illustrated in Figure 10. The vehicle is running from left side to right side with a speed of 440 km/h. When the piles are disregarded, the influence range of the velocity is quite extensive in the soils, and the Mach cone phenomenon is distinct as illustrated in Figure 10 (a). When the piles are considered, the velocity mainly affects the range of the subgrade, as shown in Figure 10 (b). The velocity of soils exhibits alternating directions: downward-upward-downward-upward, which corresponds with the position of wheelsets. Besides, it is noted that the maximum velocities of the natural and pile-reinforced ground cases are 20.93 mm/s and 19.19 mm/s, respectively, indicating the pile has a small influence on the maximum velocity of soils.

The peak particle velocity (PPV) is usually used to evaluate the dynamic influences on the surrounding environment [16, 17]. It is calculated as follows:

$$\mathrm{PPV} = \max\left|v(t)\right| \tag{4}$$

Where $v(t)$ is the time-history of the velocity of the soil.

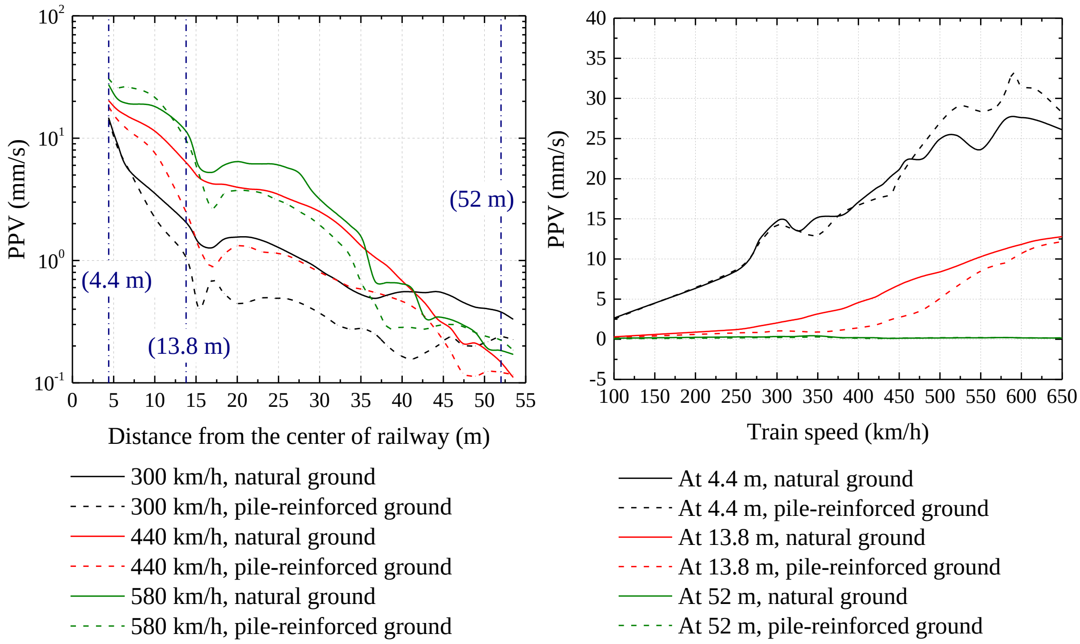

(a) PPV with distance (b) PPV with train speed

Figure 11 PPV with distance and train speed

The PPV with various distances from the center of railway under three train speeds are shown in Figure 11 (a). The PPV decreases along the overall distance. However, two amplifications which are induced by the reflections of the body waves, occur at around 20 m and 45 m. The piles can significantly reduce the PPV of soils, but the reduction effect is decreased when the train speed is increased.

The PPV with various train speeds are shown in Figure 11 (b). The PPV increases with train speed at 4.4m. The piles have no evident influence on the PPV when the train speed is lower than 300 km/h, but they slightly increase the PPV when the train speed is higher than 460 km/h. Note that the location at 4.4 m is relatively close to the center of railway, so the PPV is significantly influenced by the roughness of rail surface. The piles can considerably reduce the PPV at 13.8 m, which is located at the edge of the pile's foundation. Also, the PPV starts to increase substantially from 300 km/h in the natural ground case, but it starts to increase from 400 km/h in the pile-reinforced ground case. At 52 m, which is far away from the train-track dynamic excitation, the PPV has a small amplitude, and the piles have a minor influence on the ground vibration responses.

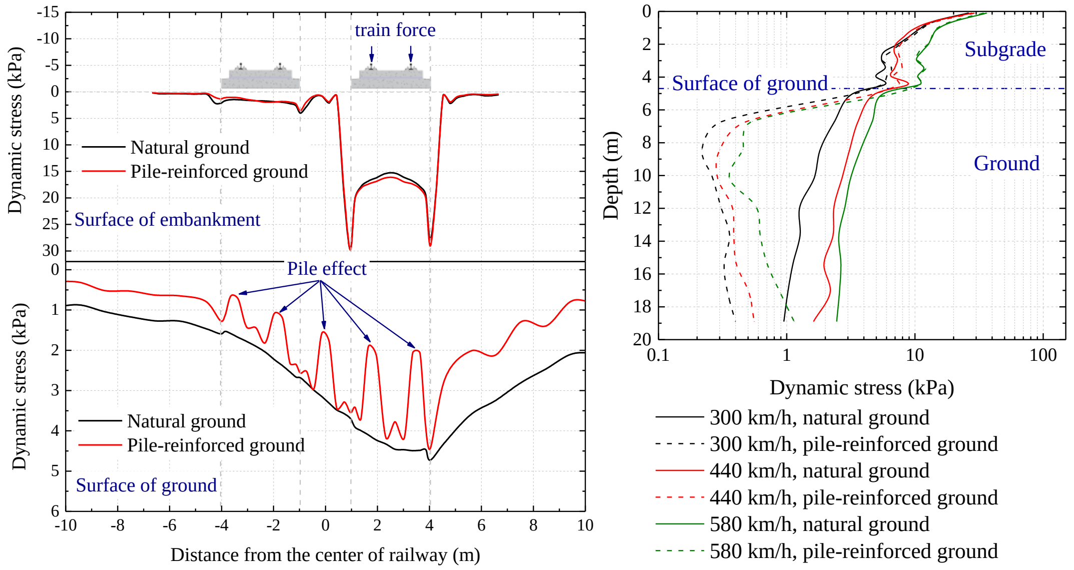

(a) Lateral distribution (b) Vertical distribution

Figure 12 Dynamic stresses of soils

The lateral distributions of the dynamic stresses at the surface of the embankment and ground are illustrated in Figure 12 (a) when the train travels at 440 km/h. The piles have no evident influence on the dynamic stresses of the embankment. The maximum dynamic stress occurs at the edge of the slab track, and a similar phenomenon can be found from Ref.[41]. However, piles can significantly reduce the dynamic stress of the ground especially when the positions are above the piles.

The attenuation effect of dynamic stress along with the depth is shown in Figure 12 (b). The dynamic stresses in the subgrade are in the range of 5 kPa to 37 kPa under three train speeds, but the piles have an insignificant influence on the stresses. In the ground, the dynamic stresses are lower than 9 kPa, and the piles can dramatically reduce the amplitudes.

4.3 Train-track interactions

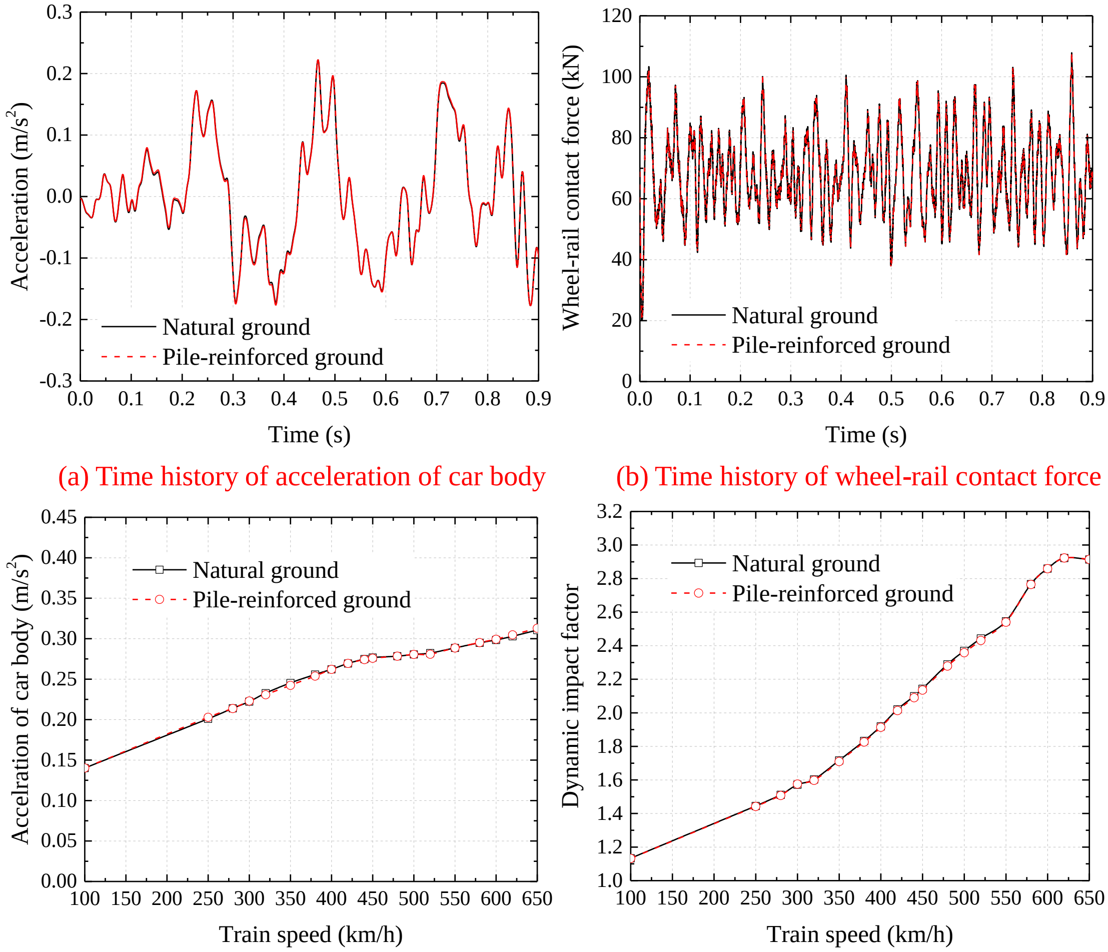

(a) Time history of acceleration of car body (b) Time history of wheel-rail contact force

(c) Acceleration of car body with train speed (d) Dynamic impact factors with train speed

Figure 13 The train-track interaction responses

Figure 13 illustrates the acceleration of the car body and the wheel-rail contact force under natural and pile-reinforced ground cases. The time history curves of acceleration of car body and wheel-rail contact force exhibit no evident difference in natural and pile-reinforced ground cases when the train speed is 300 km/h. The amplitudes of acceleration of car body and dynamic impact factors significantly increase when the train speed is increased. However, there is still no obvious difference between the results from natural and pile-reinforced ground cases, indicating the piles do not influence the train-track interactions. It is likely that the different displacement between the wheel and rail is considered too small to induce significant influences on the train-track interaction responses.

5. Discussion

It is well known that three types of waves can be generated in the soils under the dynamic excitation of the train-track-soil interactions: P wave, S wave, and Rayleigh wave. The propagation of three types of waves is complicated in the subgrade and ground in reality. In order to present an insightful and clearer wave propagation in the soils, the contours of the velocity with a train speed of 440 km/h are illustrated in Figure 14. Note that the maximum vertical velocity in the far-field (>50 m) is around 0.1 mm/s, the velocity was set to be changed from -0.1 mm/s to 0.1 mm/s to present the wave propagations in the soils including far-field. Several novel and interesting phenomena can be derived from Figure 14.

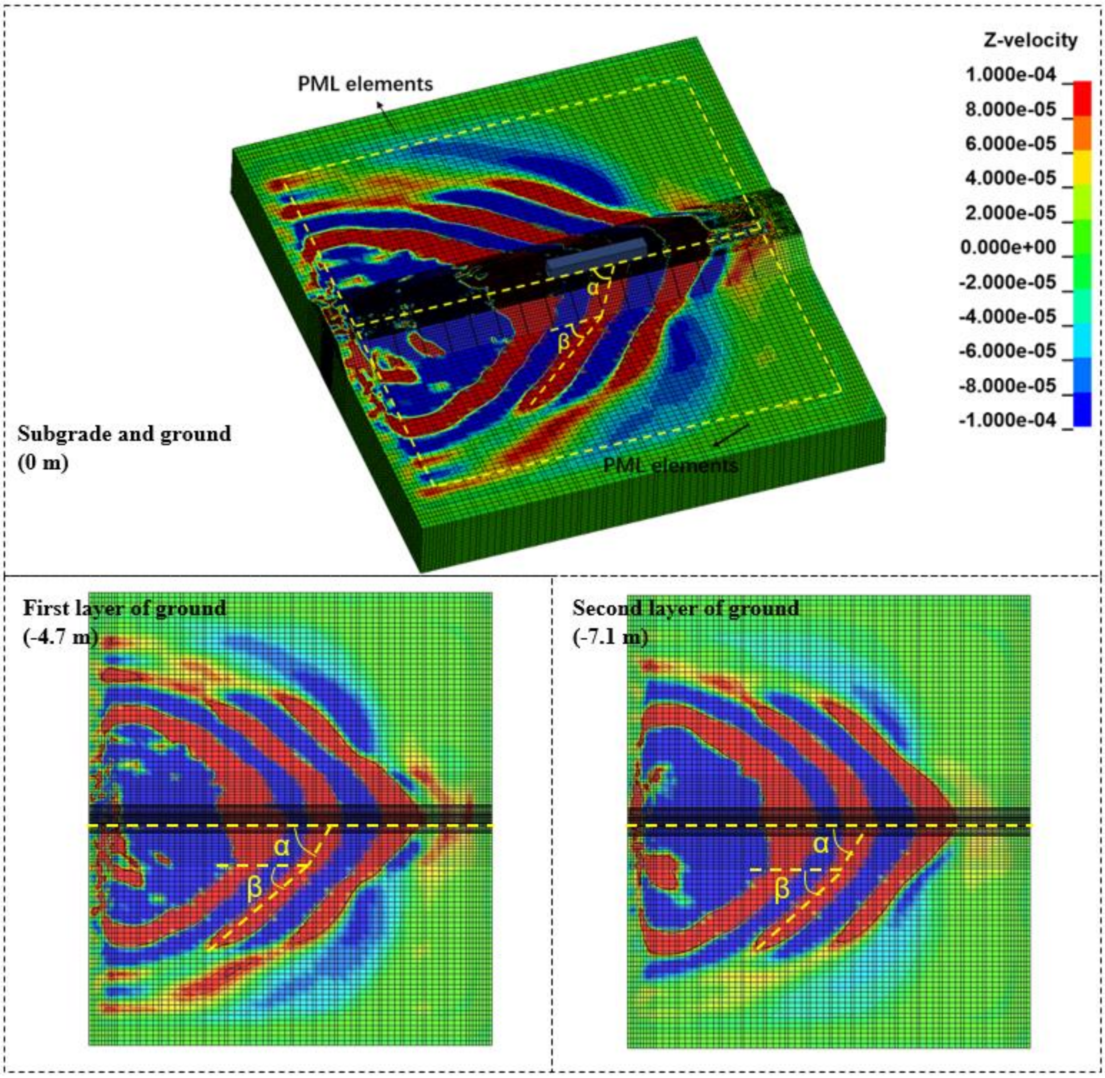

(a) Natural ground

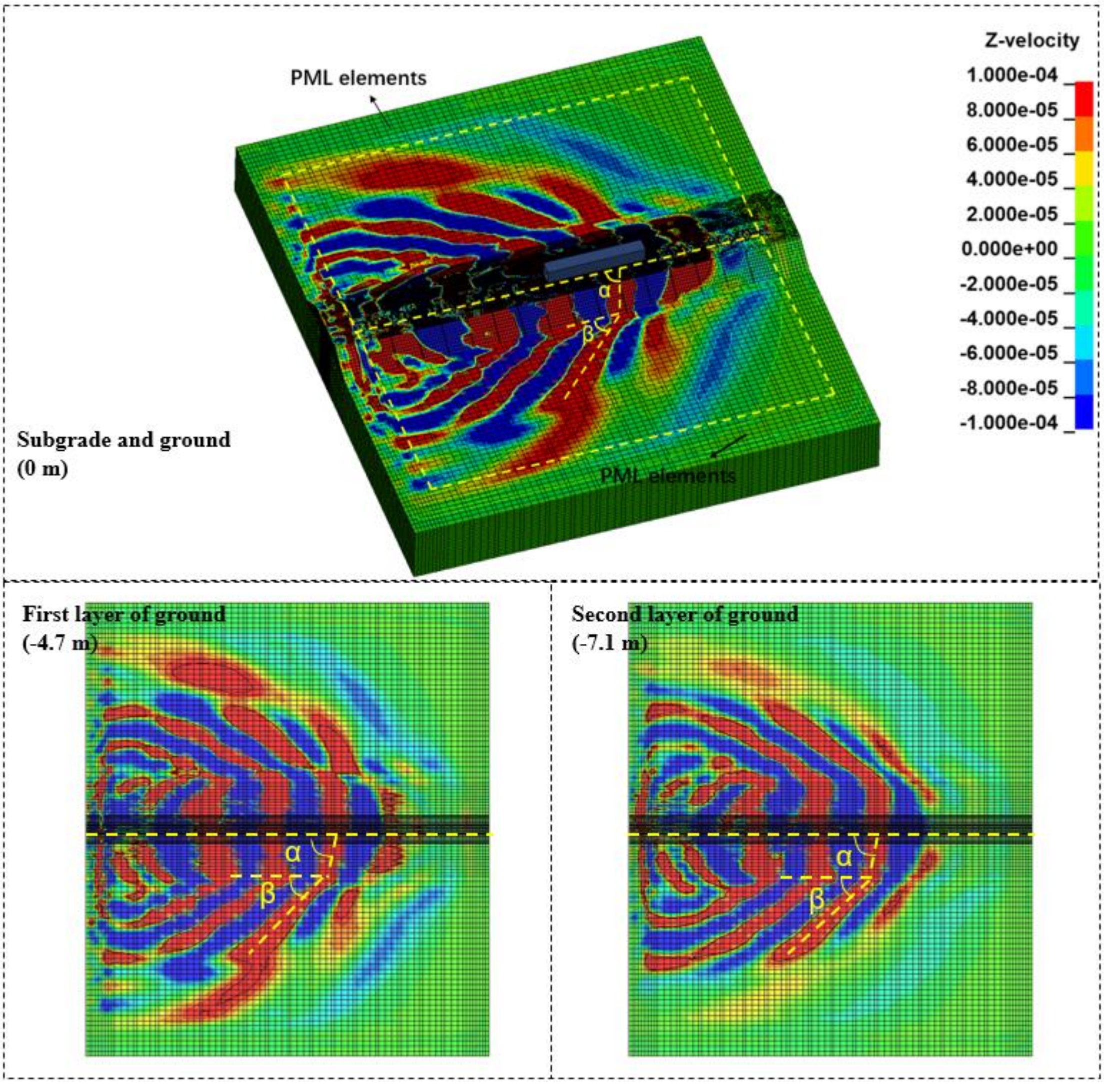

(b) Pile-reinforced ground

Figure 14 Contours of the velocity of soils

5.1 Wavelength

In the natural ground case, the three upward waves (with red color) can be observed from Figure 14 (a). However, in the pile-reinforced ground case, at least four upward waves (with red color) can be observed at the same moment. The downward waves (with blue color) exhibit the same phenomenon. Therefore, the piles can interfere with the propagation of waves and accordingly decrease the wavelength of propagation waves. To the author's knowledge, this phenomenon has never been emphasized in other researches.

5.2 Mach angles and propagation velocities

The propagation waves angles or the so-called Mach angles (α and β) in the subgrade area and ground area are measured from the top view of the figures, and the results are shown in Table 4. Note that these angles are not the same along the longitudinal direction of the railway since every wave is trying to form a circular shape after the train passes by [9], therefore one location is chosen as an example to illustrate the differences.

Table 4 Mach angles

Depth (m)	Natural ground		Pile-reinforced ground	
	α (°)	β (°)	α (°)	β (°)
0	57	-	78	-
-4.7	66	41	81	46
-7.1	66	43	81	43

The Mach angles do not remain the same with the depth of soils, as shown in Table 4. In the subgrade area, the angles (α) increase with depth from subgrade (0 m) to ground (-4.7 m and -7.1m), but the angles in the ground area (β) have no apparent difference between the two layers.

The Mach angle can be calculated as follows [9]:

$$\varphi_M = \arcsin\frac{1}{M_R} = \arcsin\frac{c_i}{v_0} \ (v_0 \geq c_i, i = P, S, \text{or } R) \tag{5}$$

Where M_R is the Mach number; c_i is the surface or body waves velocity in the soils; and v_0 is the train speed.

In the subgrade area, the dominant wave at 0 m is Rayleigh wave, but the body waves are getting decisive with depth. Since the velocities of body waves are higher than those of Rayleigh wave, the angles (α) at -4.7 m and -7.1m are higher than those at 0 m.

In the ground area, the difference of angles between two layers is relatively small. The propagation wave velocities can be re-calculated based on the measured Mach angles, as shown in Table 5. These propagation velocities are close to the Rayleigh wave velocity of the first layer of ground (307.43 km/h), so it is likely that the propagation waves are Rayleigh waves. Note that this method is not applicable to the subgrade waves since the train speed is lower than the surface or body waves velocities of subgrade.

Table 5 Propagation velocities in ground

Depth (m)	Natural ground (km/h)	Pile-reinforced ground (km/h)
-4.7	288.7	316.5
-7.1	300.1	300.1

In addition, it is noticeable that the piles can globally increase the Mach angles. Since the piles can increase the stiffness of soils, the c_i in Eq.(6) will be increased, thus the Mach angles are increased as well.

6. Conclusions

Most previous studies have considered only the natural ground vibration induced by dynamic train loads and have completely ignored the piles effects, even though the pile-reinforced ground improvement is widely adopted in high-speed railway with soft soils. In order to highlight the influences of piles on the ground vibration responses, a 3D fully coupled train-track-soil model has been developed based on the MBS principle, FEM theory, and PML method using LS-DYNA. This is thus the world's first to investigate the pile's influences on vibration responses of high-speed railway with slab tracks by a novel coupled train-track-soil model with the efficient infinite boundary of PML. Based on the dynamic responses from the models with natural and pile-reinforced grounds, the following novel insights can be drawn:

(a) High-speed railway with slab tracks exhibits a considerably high critical speed. The natural ground case has a critical speed of 440 km/h, while the pile-reinforced ground case possesses a critical speed of 580 km/h.

(b) With the improvement of piles in the ground, the dynamic responses of soils such as displacements, velocities, and stresses significantly decrease under the dynamic train loads.

(c) The train-track dynamic interaction responses are rarely influenced by the ground conditions with or without piles in the high-speed railway with slab tracks.

(d) Piles can interfere with the propagation of waves in the soils, and thus decrease the wavelength and increase the Mach angles of propagation waves.

Acknowledgments

This research was supported by the Key Research Development Program of China (No.2016YFC0802203-2, No.2016YFC0802203-3). The authors would like to acknowledge the China Scholarship Council for the financial support. The authors sincerely thank European Commission for H2020-MSCA-RISE Project No. 691135 "RISEN: Rail Infrastructure Systems Engineering Network," which enables a global research network that tackles the grand challenge in railway infrastructure resilience and advanced sensing under extreme conditions (www.risen2rail.eu).

References

[1] Remennikov AM, Kaewunruen S. A review of loading conditions for railway track structures due to train and track vertical interaction. Structural Control Health Monitoring: The Official Journal of the International Association for Structural Control and Monitoring and of the European Association for the Control of Structure. 2008;15(2):207-34.

[2] Connolly DP, Marecki GP, Kouroussis G, Thalassinakis I, Woodward PK. The growth of railway ground vibration problems—a review. Science of the Total Environment. 2016;568:1276-82.

[3] Zhai W, Han Z, Chen Z, Ling L, Zhu S. Train–track–bridge dynamic interaction: a state-of-the-art review. Vehicle System Dynamics. 2019;57(7):984-1027.

[4] Costa PA, Colaço A, Calçada R, Cardoso AS. Critical speed of railway tracks. Detailed and simplified approaches. Transportation Geotechnics. 2015;2:30-46.

[5] Li T, Su Q, Shao K, Liu J. Numerical Analysis of Vibration Responses in High-Speed Railways considering Mud Pumping Defect. Shock and Vibration. 2019;2019.

[6] Liu K, Su Q, Yue F, Liu B, Qiu R, Liu T. Effects of suffosion-induced contact variation on dynamic responses of saturated roadbed considering hydro-mechanical coupling under high-speed train loading. Computers and Geotechnics. 2019;113:103095.

[7] Feng S-J, Zhang X-L, Wang L, Zheng Q-T, Du F-L, Wang Z-L. In situ experimental study on high speed train induced ground vibrations with the ballast-less track. Soil Dynamics and Earthquake Engineering. 2017;102:195-214.

[8] Connolly DP, Kouroussis G, Laghrouche O, Ho C, Forde M. Benchmarking railway vibrations–Track, vehicle, ground and building effects. Construction and Building Materials. 2015;92:64-81.

[9] Kouroussis G, Connolly DP, Verlinden O. Railway-induced ground vibrations–a review of vehicle effects. International Journal of Rail Transportation. 2014;2(2):69-110.

[10] Thompson DJ, Kouroussis G, Ntotsios E. Modelling, simulation and evaluation of ground vibration caused by rail vehicles. Vehicle System Dynamics. 2019;57(7):936-83.

[11] Huang H, Chrismer S. Discrete element modeling of ballast settlement under trains moving at "Critical Speeds". Construction and Building Materials. 2013;38:994-1000.

[12] Sheng X, Jones C, Thompson D. A theoretical study on the influence of the track on train-induced ground vibration. Journal of Sound and Vibration. 2004;272(3-5):909-36.

[13] Hall L. Simulations and analyses of train-induced ground vibrations in finite element models. Soil Dynamics and Earthquake Engineering. 2003;23(5):403-13.
[14] Dong K, Connolly DP, Laghrouche O, Woodward P, Costa PA. Non-linear soil behaviour on high speed rail lines. Computers and Geotechnics. 2019;112:302-18.
[15] Shih J-Y, Thompson DJ, Zervos A. The influence of soil nonlinear properties on the track/ground vibration induced by trains running on soft ground. Transportation Geotechnics. 2017;11:1-16.
[16] Kouroussis G, Verlinden O, Conti C. Influence of some vehicle and track parameters on the environmental vibrations induced by railway traffic. Vehicle System Dynamics. 2012;50(4):619-39.
[17] Kouroussis G, Conti C, Verlinden O. Investigating the influence of soil properties on railway traffic vibration using a numerical model. Vehicle System Dynamics. 2013;51(3):421-42.
[18] Olivier B, Connolly DP, Alves Costa P, Kouroussis G. The effect of embankment on high speed rail ground vibrations. International Journal of Rail Transportation. 2016;4(4):229-46.
[19] Zhai W, Wei K, Song X, Shao M. Experimental investigation into ground vibrations induced by very high speed trains on a non-ballasted track. Soil Dynamics and Earthquake Engineering. 2015;72:24-36.
[20] Zheng G, Jiang Y, Han J, Liu Y-F. Performance of cement-fly ash-gravel pile-supported high-speed railway embankments over soft marine clay. Marine Georesources and Geotechnology. 2011;29(2):145-61.
[21] Lai J, Liu H, Qiu J, Chen J. Settlement analysis of saturated tailings dam treated by CFG pile composite foundation. Advances in Materials Science Engineering. 2016;2016.
[22] You S, Cheng X, Guo H, Yao Z. Experimental study on structural response of CFG energy piles. Applied Thermal Engineering. 2016;96:640-51.
[23] Chen Q-n, Zhao M-h, Zhou G-h, Zhang Z-h. Bearing capacity and mechanical behavior of CFG pile composite foundation. Journal of Central South University of Technology. 2008;15(2):45-9.
[24] Kaewunruen S, Wang Y, Ngamkhanong C. Derailment-resistant performance of modular composite rail track slabs. Engineering Structures. 2018;160:1-11.
[25] Kaewunruen S, Remennikov AM. Current state of practice in railway track vibration isolation: an Australian overview. Australian Journal of Civil Engineering. 2016;14(1):63-71.
[26] Kaewunruen S, Kimani SK. Damped frequencies of precast modular steel-concrete composite railway track slabs. Steel and Composite Structures. 2017;25(4):427-42.
[27] Thach P-N, Liu H-L, Kong G-Q. Vibration analysis of pile-supported embankments under high-speed train passage. Soil Dynamics and Earthquake Engineering. 2013;55:92-9.
[28] Tang Y, Xiao S, Yang Q. Numerical study of dynamic stress developed in the high speed rail foundation under train loads. Soil Dynamics and Earthquake Engineering. 2019;123:36-47.
[29] Connolly D, Giannopoulos A, Forde M. Numerical modelling of ground borne vibrations from high speed rail lines on embankments. Soil Dynamics and Earthquake Engineering. 2013;46:13-9.
[30] Connolly D, Kouroussis G, Giannopoulos A, Verlinden O, Woodward P, Forde M. Assessment of railway vibrations using an efficient scoping model. Soil Dynamics and Earthquake Engineering. 2014;58:37-47.
[31] Wang M, Cai C, Zhu S, Zhai W. Experimental study on dynamic performance of typical nonballasted track systems using a full-scale test rig. Proceedings of the Institution of Mechanical Engineers, Part F: Journal of Rail and Rapid Transit. 2017;231(4):470-81.
[32] Lei X, Wang J. Dynamic analysis of the train and slab track coupling system with finite elements in a moving frame of reference. Journal of Vibration and Control. 2014;20(9):1301-17.

[33] Li T, Su Q, Kaewunruen S. Saturated Ground Vibration Analysis Based on a Three-Dimensional Coupled Train-Track-Soil Interaction Model. Applied Sciences. 2019;9(23):4991.

[34] Li T, Kaewunruen S, Su Q, Goto K. Effects of static and dynamic material properties on vibration responses of slab tracks in high speed railways. ACOUSTICS 2019. Milton Keynes, United Kingdom: Proceedings of the Institute of Acoustics, 2019. p. 246-54.

[35] Basu U. Explicit finite element perfectly matched layer for transient three- dimensional elastic waves. International Journal for Numerical Methods in Engineering. 2009;77(2):151-76.

[36] Wang J, Jin X, Cao Y. High-speed maglev train-guideway–tunnel–soil modelling of ground vibration. Proceedings of the Institution of Mechanical Engineers, Part F: Journal of Rail and Rapid Transit. 2012;226(3):331-44.

[37] You R, Goto K, Ngamkhanong C, Kaewunruen S. Nonlinear finite element analysis for structural capacity of railway prestressed concrete sleepers with rail seat abrasion. Engineering Failure Analysis. 2019;95:47-65.

[38] Lee C, Bolton M, Al-Tabbaa A. Numerical modelling of group effects on the distribution of dragloads in pile foundations. Geotechnique. 2002;52(5):325-35.

[39] Shengcai Y. Calculation and Assessment Analysis of the Dynamic Performance for Slab Track on Sui-Yu Railway. Chengdu: Southwest Jiaotong University, 2007.

[40] Cai C, Zhai W, Wang K. Calculation and Assessment Analysis of the Dynamic Performance for Slab Track on Sui-Yu Railway. China Railway Science. 2006;04:17-21.

[41] Hu J, Bian X, Xu W, Thompson D. Investigation into the critical speed of ballastless track. Transportation Geotechnics. 2019;18:142-8.